論文 / 著書情報
Article / Book Information

Title	Apo-ferritin-Caged Pt Nanoparticles for Selective Hydrogenation of p-Chloronitrobenzene
Authors	Yinhuan Zhou, Yilin Zheng, Chenlin Lu, Basudev Maity, Yakui Chen, Takafumi Ueno, Zheng Liu, Diannan Lu
Citation	ACS Applied Nano Material, Vol. 6, Issue 7, Page 5835-5843
Pub. date	2023, 4
Note	This document is the Accepted Manuscript version of a Published Work that appeared in final form in ACS Applied Nano Material, copyright (c) American Chemical Society after peer review and technical editing by the publisher.To access the final edited and published work see https://doi.org/10.1021/acsanm.3c00231.
Note	This file is author (final) version.

Apo-ferritin Caged Pt Nanoparticles for Selective Hydrogenation of *p*-Chloronitrobenzene

Yinhuan Zhou [a], *Yilin Zheng* [b], *Chenlin Lu* [a], *Basudev Maity* [c], *Yakui Chen* [a], *Takafumi Ueno* [*c, d], *Zheng Liu* [a], *and Diannan Lu* [*a]

[a]*Department of Chemical Engineering, Tsinghua University, Beijing 100084, China. E-mail: zhou-yh20@mails.tsinghua.edu.cn, lucl17@outlook.com, chenyk21@mails.tsinghua.edu.cn, liuzheng@tsinghua.edu.cn, ludiannan@tsinghua.edu.cn.*

[b]*Institute of Biopharmaceutical and Health Engineering, Shenzhen International Graduate School, Tsinghua University, Shenzhen 518055, China. zhengyl22@mails.tsinghua.edu.cn.*

[c] *School of Life science and Technology, Tokyo Institute of Technology, Nagatsuta-cho 4259, Midori-ku, Yokohama 226-8501, Japan, Email: basudev@bio.titech.ac.jp, tueno@bio.titech.ac.jp.*

[d]*Living Systems Materialogy (LiSM) Research Group, International Research Frontiers Initiative (IRFI), Tokyo Institute of Technology, Nagatsuta-cho 4259, Midori-ku, Yokohama 226-8501, Japan, Email: tueno@bio.titech.ac.jp.*

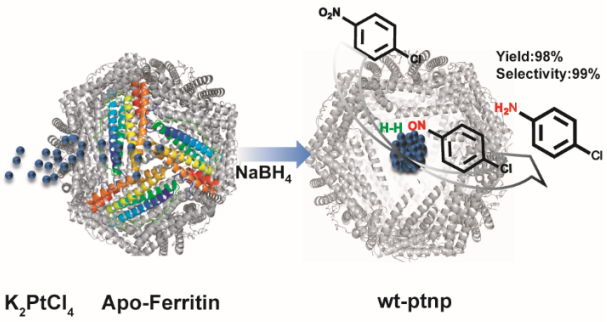

ABSTRACT: Reducing halogenated nitrobenzenes to the corresponding halogenated anilines is a critical process in the production of chemical industries. However, commonly used metal catalysts often require high temperatures and pressurized hydrogen during synthesis and catalysis and are prone to dehalogenation reactions with low selectivity of the reaction. Here we synthesize size-controlled (1.8-3 nm) apo-ferritin-caged Pt nanoparticles at room temperature.

The catalysts can efficiently convert p-chloronitrobenzene to p-chloroaniline at 50℃ for 30 min and effectively inhibit dechlorination reaction with a selectivity of up to 99%, the TOF (22.8 min^{-1}) is nearly ten times higher than that of the unloaded platinum nano-catalyst. In addition, the catalysts also show a selectivity higher than 90% for another halogenated nitrobenzene. The TEM and XPS results reveal that the unique size effect and the electronic effect of the catalyst due to the interaction between apo-ferritin and platinum is a significant reason for its performance enhancement, which also provides some theoretical basis for the rational design of protein-based metal nano-catalysts.

KEYWORDS. Pt nanoparticles, apo-ferritin, high selectivity, halogenated nitrobenzene, hydrogenation reduction

INTRODUCTION

Halogenated aromatic amines are essential intermediates[1] for medicine, fiber, dye, rubber, and other fields[2], obtained through hydrogenation of halogenated nitrobenzenes catalyzed by metal, sulfide, and electrolysis[3-6]. However, the hydrogenation reaction catalyzed by the metal catalyst and alkali sulfide produces metal sludge and sulfur-containing benzene wastes[6]. In contrast, those by the electrolytic method suffer from energy consumption and equipment requirements[4]. The above catalytic reaction methods are adequate for converting simple nitroaromatic hydrocarbons to aromatic amines, but the selectivity could be better for halogenated nitrobenzenes. The main reason is that the hydrogenation-reduction process of halogenated nitrobenzenes is a very complex reaction, including several parallel and stepwise reaction processes, which generates by-products and intermediate substances such as aniline, azo substances, and hydroxylamine, which will affect the yield of halogenated aniline[7-10]. Although there have been many studies on the reduction reactions of halogenated aromatic hydrocarbons, few have achieved the desired catalytic effect, and many catalysts still have low activity or selectivity. Therefore, how to control the catalyst to hydrogenate only the nitro group without involving the removal of halogen substituents and still improve the selectivity and reduce the accumulation of by-products based on its high activity is a complex problem for this reaction.

The most applied method to solve this reaction problem is catalytic hydrogenation

by metal nanocatalysts. Hydrogenation using non-noble metal catalysts is an environmentally friendly procedure[5,11-15]. Pogorelic *et al.*[16] examined the workability of Raney Ni in the hydrogenation of various aromatic nitro compounds and found the activity and selectivity of the catalyst were not satisfactory, leading to the accumulation of intermediates in terms of N-phenylhydroxylamine and azo compound reaction[17,7-9]. Gold and silver catalysts have high position selectivity for hydrogenation but low activity, whereas Pt and Pd catalysts have high activity but low selectivity[18-20]. Loaded noble metal nanocatalysts are also the most common and effective method for the selective reduction of halogenated nitrobenzene[21]. Qiaoqiao Guan *et al.*[22] prepared bimetallic monolayer catalysts loaded on SiO_2 by atomic layer deposition ALD method to catalyze the reaction of chloronitrobenzene with Au@1ML-Pt of different sizes, which achieved highly selective conversion of p-chloronitrobenzene at 65°C and 0.3 MPa H_2. The introduction of another noble metal in this study improved the reaction activity and selectivity but also made the preparation process more tedious and increased the cost. In addition, the preparation and reaction of the catalyst in this study were carried out under high temperature and pressure conditions, so the method requires a relatively high preparation process and production process of the catalyst. Miaomiao Liu *et al.*[23] synthesized Pt-SnO_2 hybrid nanocatalysts by in situ transformation of Pt@Sn core-shell nanoparticles and investigated their catalytic performance for the hydrogenation of various substituted nitroaromatics, which improved the selectivity of chlorinated anilines to 86.9% by reacting at 45°C, and 0.1 MPa H_2 for one hour. In addition, there are also many kinds of research on Rh, Pd, Ag, Ru, and other noble metal catalysts[24-27] for catalyzing hydrogenation. The noble metal nanocatalyst hydrogenation method is more efficient and environmentally friendly than the chemical reduction method. However, the synthesis and reaction of the catalyst in this method often need to be carried out under high temperature and high-pressure conditions, which requires high equipment requirements[25]. In addition, these metal nanocatalysts are prone to agglomeration during the synthesis and catalysis process, so substances such as stabilizers need to be added to assist the synthesis of the catalyst, which can affect the catalyst activity to some extent. Usually, when preparing these loaded metal nanocatalysts, removing these substances by other methods as much as

possible is necessary to ensure the catalyst's performance. Therefore, eliminating the influence of other substances to ensure the stability and efficiency of metal nanoparticles is also a challenge in metal nano catalytic applications[21, 28-32].

How to prepare highly selective catalysts that can solve the problems of low selectivity of halogenated nitrobenzene reaction, complicated synthesis process of traditional metal nanocatalysts, and unstable catalysts by simple methods is also a problem that we hope to solve in our research. Here we try to synthesize metal nanocatalysts using protein as a carrier under mild conditions with the help of the concept of biomineralization while achieving stabilization of metal nanoparticles with the help of the domain-limited space of proteins[33-35]. The catalyst constructed by this method combines properties such as the high activity of metal nanocatalysts and the chiral environment of the protein backbone. As a result, it may improve the selectivity of halogenated nitrobenzene hydrogenation reduction reactions under mild conditions. Furthermore, compared with the current method of synthesizing metal nanocatalysts by high-temperature calcination with relatively cumbersome conditions[23], we can prepare water-soluble and stable metal nanocatalysts by simple mixing and stirring at

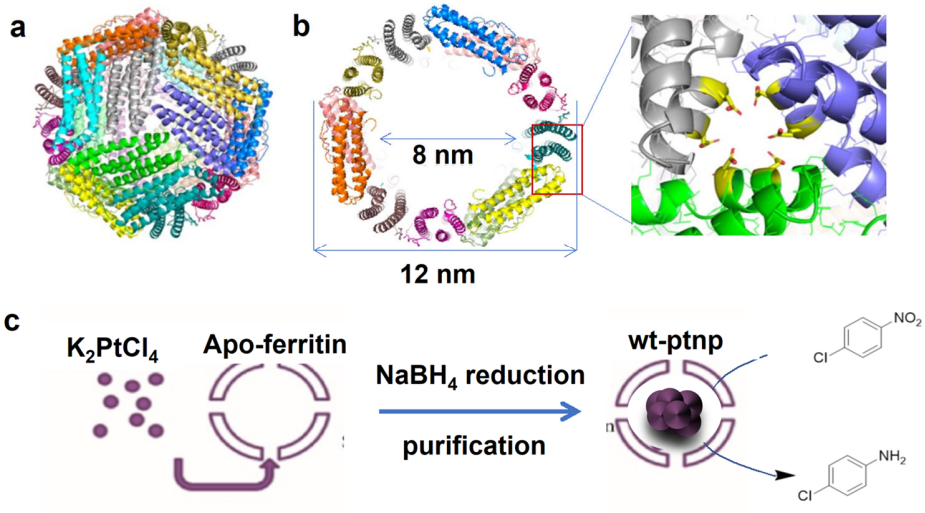

Figure 1. a Overall 24-mer cage structure of the ferritin cage. **b** Interior cavity of the ferritin cage showing a 3-fold pore through which metal ions can diffuse into the cage. Protein structure was prepared in pymol using pdb code 1dat. **c** Schematic representation of the preparation of PtNP in ferritn cage and catalytic reduction of *p*-chloronitrobenzene.

room temperature. As a result, the preparation and reaction conditions are milder, less energy-consuming, and safer.

Ferritin is a 480 kDa spherical cage-like protein with an outer diameter of 12 nm and an inner diameter of 8 nm. It has eight hydrophilic channels located in the triploid axis and six hydrophobic channels located in the quadrupled axis (Figure 1a, b). Metal ions enter the cage mainly through the triploid axis hydrophilic channels [36], also available for reactants, thereby imposing a size-selective effect on reactants[37]. Yan *et al.*[38] loaded Fe_3O_4 particles into human heavy-chain ferritin and found its activity in catalyzing oxidation using hydrogen peroxide. The ferritin cage can separate the internal and external environment, effectively prevent the aggregation of nanoparticles, improve particle stability, and is beneficial to the preparation of small-size nanoparticles[39]. Small nanoclusters are always the most active due to their large surface area and having atom-like properties than large nanoparticles[40]. Moreover, the nanocluster in the ferritin cage becomes water-soluble and stable[41]. The confined protein environment can give additional advantages in controlling the catalytic reactions controlled by nanocluster[42]. Controlling the structure of ferritin metal nanoparticles by adjusting the conditions of ferritin and metal reduction reaction is expected to enhance their catalytic selectivity[33, 37, 39, 43-44].

Considering the protein channel selectivity and the unique size effect of metal nanoparticles, we chose ferritin as a carrier. We tried to mix different ratios of protein and platinum by simple diffusion and reduce them to different sizes of platinum metal nanoparticles with the help of sodium borohydride. We expect to construct stable metal nanocatalysts suitable for the selective conversion of *p*-chloronitrobenzene (Figure 1c) by this simple method to solve the complex problem of low selectivity of this reaction and also to expand the range of substrate spectrum of this catalyst, and finally, we also explore the catalytic mechanism with the information of morphological structure and electronic structure of the catalyst.

EXPERIMENTS AND METHODS

Preparation of Pt nanoparticles caged in apo-ferritin. 5 mL of a 5 μM solution of apo-ferritin (recombinant horse spleen L-ferritin) and different volumes of 10 mM of K_2PtCl_4 in 50 mM Tris-HCl (pH 8.0)/0.15 M NaCl were stirred and mixed at room temperature for two hours and followed by the 0.5 h reduction using $NaBH_4$ solution. To prevent aggregation, we freshly purified our ferritin and dissolved it in a 50 mM Tris-HCl-0.15 M

NaCl buffer at pH 8 without any additional pH adjustment, thereby avoiding any further increase in salt concentration. The state of the ferritin and buffer conditions greatly affect its stability, and our use of purified ferritin allowed it to react with more platinum metal in our reaction system without any precipitation, in contrast to the previous study[35]. Next, the solution was stirred and dialyzed in 50 mM Tris-HCl (pH 8.0)/0.15 M NaCl for 12 hours, filtered by 0.22 μm filter membrane, further desalted and purified by desalting column, yielding Pt nanoparticles caged in apo-ferritin in 50 mM Tris-HCl (pH 8.0)/0.15 M NaCl (Figure. S1).

The electrophoresis results show that the skeleton structure of the apo-ferritin has not changed (Figure. S2). K_2PtCl_4 of different concentrations were added to apo-ferritin yielding apo-ferritin caged Pt catalyst of different Pt content, namely wt-ptnp1000, wt-ptnp5000, and wt-ptnp10000, in which the molar ratio of Pt ion to apo-ferritin is 1000, 5000, and 10000, respectively.

Method of characterization of apo-ferritin caged Pt. The Pt content in wt-ptnp was determined quantitatively by inductively coupled plasma mass spectrometry (ICP-MS Agilent 5110). The protein concentration was measured by BCA (bicinchoninic acid) method. The morphology of wt-ptnp (4.2 μM) was characterized by transmission emission microscopy (TEM) (FEI talos F200x G2) and X-ray photoelectron spectroscopy (Thermo Scientific K-Alpha) and treated with XPSPEAK41. The appropriate experimental methods are shown in the supporting information.

Method of catalytic reaction. We use wt-ptnp and ptnp to catalyze the hydrogenation of *p*-chloronitrobenzene (*p*-CNB) to *p*-chloroaniline (*p*-CAN), detailed in SI. After the reaction, the product was extracted with *n*-hexane and used for GC-MS analysis (Agilent 7890B-7000D). The conversion *X*, selectivity *S* and the turnover frequency (TOF) of the apo-ferritin caged Pt are determined as follows

$$X(\%) = 1 - \frac{n_{(p-\mathrm{CNB})}}{n_{0(p-\mathrm{CNB})}} \times 100\% \quad (1)$$

$$S(\%) = \frac{n_{(p-\mathrm{CNA})}}{n_{0(p-\mathrm{CNB})} - n_{(p-\mathrm{CNB})}} \times 100\% \quad (2)$$

$$\mathrm{TOF}(\mathrm{min}^{-1}) = \frac{n_{(p-\mathrm{CNA})}}{n_{Pt} \times t} \quad (3)$$

In which $n_{0(p\text{-CNB})}$ is the initial molar number of *p*-chloronitrobenzene, $n_{(p\text{-CNB})}$ is the final molar content of *p*-chloronitrobenzene, $n_{(p\text{-CNA})}$ is the molar content of *p*-chloroaniline, n_{Pt} is the molar content of Pt, and t is time(minute).

RESULTS AND DISCUSSION

Characterization of apo-ferritin caged Pt catalysts. Table 1 lists the apo-ferritin caged Pt catalysts(wt-ptnp) prepared in the present study. The three data sets plotted as Pt/wt values against the initial addition of Pt equivalents show a linear relationship (Figure.S3). For example, when reacted with 1000 equiv, 19 Pt bounded to apo-ferritin.

Table 1. Quantitative estimation of Pt content in wt-ptnp.

wt-ptnp	wt (μmol/L)	Pt (μmol/L)	Pt/wt
wt-ptnp1000[a]	0.61	11.88	19±1
wt-ptnp5000[a]	0.60	29.83	49±1
wt-ptnp10000[a]	0.76	66.94	88±1

[a] 1000, 5000 and 10000 represent the number of equivalents of K_2PtCl_4 (Pt) with respect to apo-ferritin (wt) used for the preparation of wt-ptnp.

The number can increase to 88 per cage with the increase of Pt equivalents, which is interesting because we can control the metal loading efficiency of apo-ferritin and indirectly affects the size of the nanoparticles formed inside the cage, which ultimately reflects in the activity of nanomaterials. In addition, the electrophoresis results showed that the overall structure of the apo-ferritin cage in wt-ptnp remained unchanged after the reaction (Figure. S2).

The TEM image of the wt-ptnp (Figure.2 c-f) clearly shows apo-ferritin-caged Pt particles are spherical in morphology and are better dispersed, smaller, and more uniform in size than Pt particles reduced directly in solution (about 35 nm) in Figure.2, which is because small nanoclusters tend to aggregate in solution. If the Pt nanoparticles were on the outer surface of the ferritin, they would be aggregated into large size particles, rather than the small size nanoparticles in our experimental results. At the same time, the closed environment of the apo-ferritin cage prevents them. In addition, the 8 nm cavity of apo-ferritin provides a good domain-limited space for the synthesis of small-sized Pt nanoparticles, which makes the synthesized Pt nanoparticles less prone to aggregation and form particles smaller than 8 nm (Figure 2c and Figure S4). The HR-TEM images show that the Pt particles of wt-ptnp1000 and 5000 have a smaller average particle size with 1.8 nm and 2.2 nm compared to 3.1 nm of wt-ptnp10000 in Figure. 2 d-f. Accordingly, the size of the Pt nanoparticles synthesized in ferritin

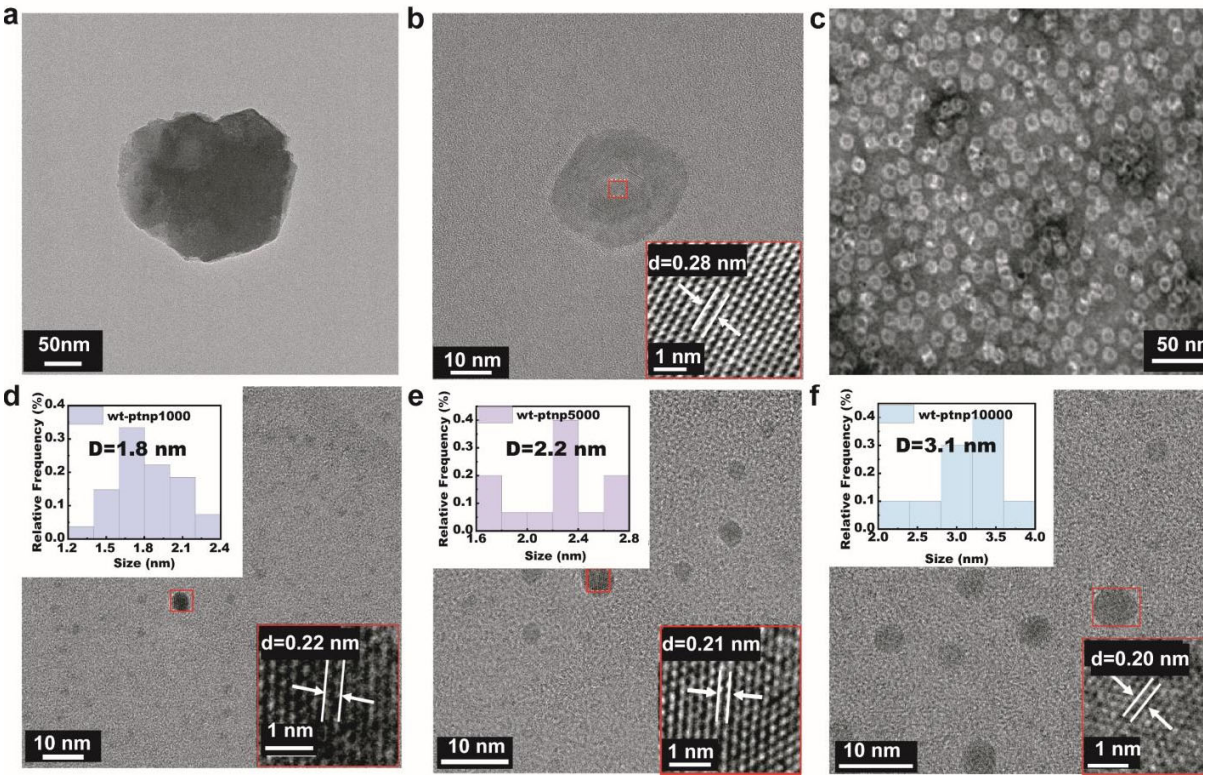

Figure 2. Morphological characterization of ptnp and wt-ptnp. **a** TEM image of ptnp (K_2PtCl_4 reduced by $NaBH_4$) under scale of 50 nm, **b** TEM images of ptnp (K_2PtCl_4 by $NaBH_4$) under scale of 10 nm, **c** the negative staining of wt-ptnp1000, **d** TEM images of wt-ptnp1000, **e** TEM images of wt-ptnp5000, **f** TEM images of wt-ptnp10000. The upper left illustration of **d-f** is a statistical graph of particle size and the lower right inset of **d-f** is an HRTEM image of the region indicated by the box. Diameter was measured by Image J software.

increases with the increase in Pt content. Since the catalyst preparation and detection is not in an inert gas, oxygen may be introduced on the surface of the platinum nanoparticles to produce platinum oxide substances, so the presence of platinum oxide substances will be detected. Moreover, we found that the crystal plane distance of the ptnp (K_2PtCl_4 reduced by $NaBH_4$) is about 0.28 nm, corresponding to the (100) crystal plane of PtO[45](Figure.S4). When 1000, 5000, and 10000 times the amount of Pt was added to apo-ferritin, the crystal plane distance of the catalysts, wt-ptnp1000, wt-ptnp5000, and wt-ptnp10000, was approximately 0.22, 0.21, and 0.20 nm, respectively, which are

much smaller than the crystal plane distance of the ptnp (K_2PtCl_4 reduced by $NaBH_4$). Furthermore, the crystal plane of wt-ptnp1000, wt-ptnp5000, and wt-ptnp10000 are (220) of PtO[46] (the lower right inset of Figure.2 d-f and Figure.S4), respectively[47]. These results suggest that the size of the Pt nanoparticles caged in apo-ferritin can be adjusted by the amount of Pt added during the preparation process.

Figure. 3 gives XPS analysis of ptnp, wt-ptnp1000, wt-ptnp5000, and wt-ptnp10000. According to the peak energy position and peak characteristics of the Pt4f spectrum, the $Pt4f_{7/2}$ peak of wt-ptnp1000 and 5000 can be fitted with three components which are assigned to metallic Pt (0), Pt (II), and Pt (IV) [29, 33, 48] At the same time, the Pt in wt-ptnp10000 and ptnp contained Pt (0) and Pt (II) but no Pt (IV). We believe that the emergence of Pt (IV) can be attributed to two possible reasons. Firstly, it is possible that oxygen was introduced during the preparation and testing of wt-ptnp, causing the surface platinum to oxidize and display a tetravalent state. Secondly, there may be some platinum

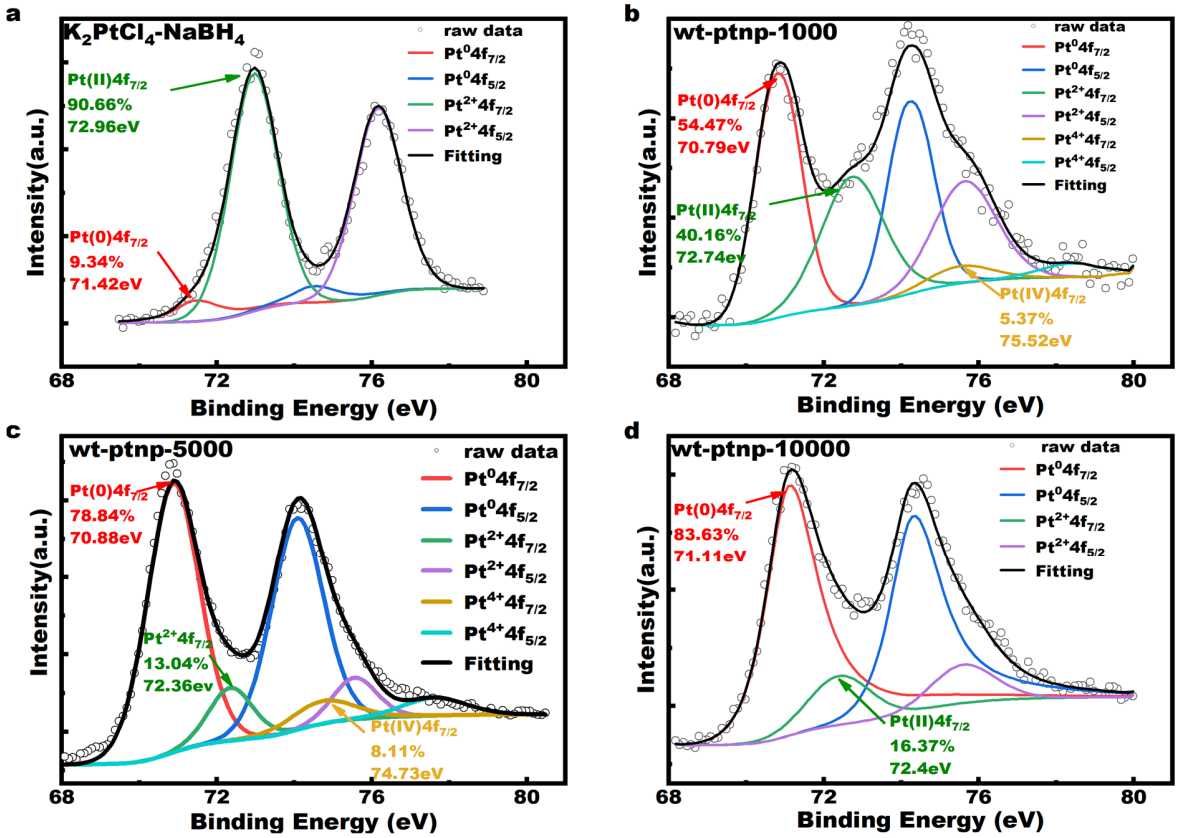

Figure 3. XPS spectral characterization. Pt 4f XPS spectra of **a** ptnp(K_2PtCl_4-$NaBH_4$), **b** wt-ptnp1000, **c** wt-ptnp5000, **d** wt-ptnp10000.

coordinated with ferritin in the prepared wt-ptnp that was not reduced during the preparation process. As a result, wt-ptnp1000 and wt-ptnp5000 contain tetravalent platinum due to coordination reasons, leading to the detection of Pt (IV) during XPS analysis. In addition, there is a significant difference in the amount of Pt in the different valence states of these catalysts, with wt-ptnp1000 containing 54.47 % Pt (0), wt-ptnp5000 containing 78.84 % Pt (0), and wt-ptnp10000 containing 83.63 % of Pt (0), which shows that the proportion of Pt (0) increases and the shifting of Pt4f binding energy towards the lower-energy side diminishes with increasing Pt content and Pt particle size[33, 47-50]. The significant difference in the Pt binding energy between the wt-ptnp and ptnp catalysts may be attributed to the electronic structure change of Pt through the metal-carrier interactions between Pt and apo-ferritin[30].

Catalytic hydrogenation of *p*-chloronitrobenzene. The geometrical diameter of the ferritin triplet channel is approximately 5.0 Å, while the interatomic distance between the two hydrogen atoms in *p*-chloronitrobenzene is about 4.3 Å. Previous studies have demonstrated that molecules smaller than 5.0 Å can pass through the triplet channel[3]. Furthermore, Prastaro *et al*[44] have reported the Suzuki-Miyaura coupling reaction of 4-Iodobenzoic acid with 2-tolylboronic acid inside the ferritin cage. Given the similarity in size between *p*-chloronitrobenzene and 4-Iodobenzoic acid, we propose that *p*-chloronitrobenzene can enter the ferritin triplet channel and the ferritin cage.

Hydrogenation of *p*-chloronitrobenzene (*p*-CNB) using the synthesized Pt nanoparticles caged in apo-ferritin and the Pt control catalyst was conducted, as detailed in supporting information. The reaction was performed in an aqueous medium at 50℃ in the presence of $NaBH_4$ for 30-60 min. After hydrogenation, the *p*-chloronitrobenzene converts into *p*-chloroaniline and the corresponding dechlorinated product, aniline (Figure 4). The control Pt catalyst converted 93% of the substrate and formed *p*-chloroaniline with only 60% selectivity. In contrast, the wt-ptnp1000, wt-ptnp5000, and wt-ptnp10000 converted over 98% and a significantly higher selectivity of over 99% for the formation of *p*-chloroaniline (Figure. 4 a). The above results suggest the role of the protein environment in catalysis, which gave only the particular *p*-chloroaniline product compared to the free Pt control catalyst, which gave a mixture of products (Figure.5a). The increased substrate concentration reduced conversion and yield, whereas the product

selectivity remained unchanged (Figure 4b, c). The limited catalytic surface might cause such a decrease in the conversion/yield at high substrate concentration. Interestingly, the caged Pt catalyst maintained high selectivity even at high substrate concentrations.

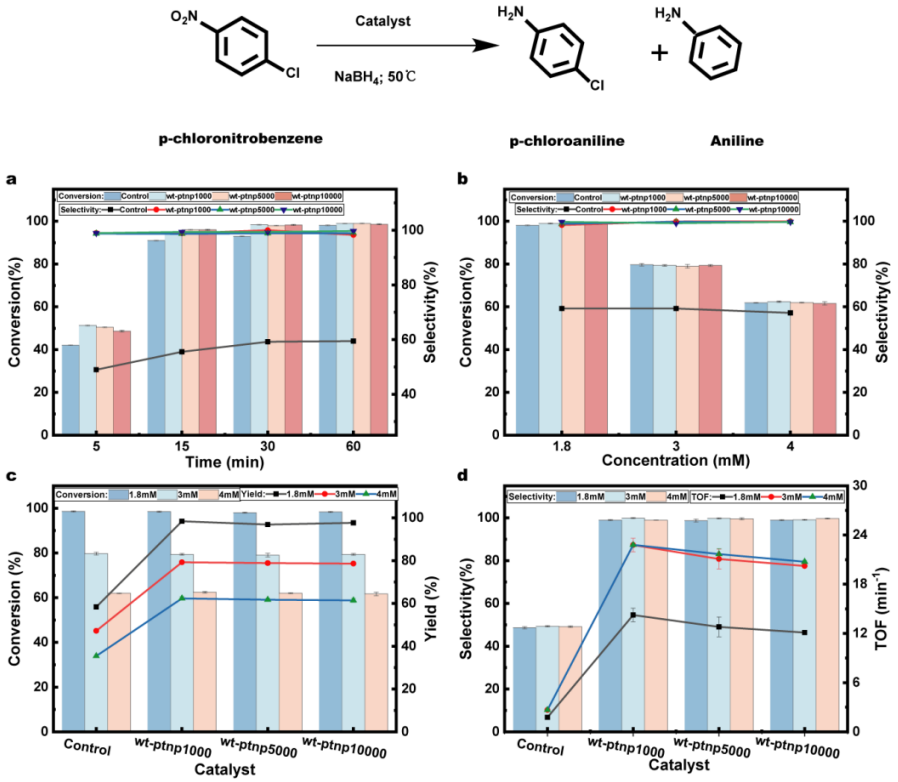

Figure 4. Evaluation of the catalytic reduction of *p*-chloronitrobenzene(*p*-CNB) into selective *p*-chloroaniline (*p*-CAN) product by control group (ptnp) and wt-ptnp catalysts. **a** the conversion and selectivity at different time intervals. Reaction conditions: Catalyst (0.88 μM), *p*-chloronitrobenzene (1.8 mM), $NaBH_4$ (20 mM), 50°C**. b** the conversion and selectivity under different concentrations. Reaction conditions: Catalyst (0.88 μM), *p*-chloronitrobenzene (1.8 mM /3 mM /4 mM), $NaBH_4$ (20 mM), 50°C and 1 h**. c** the catalytic conversion and yield for different catalysts at different substrate concentrations. Reaction conditions is same as **b. d** the selectivity and TOF for different catalysts at different substrate concentrations. Reaction conditions: Catalyst (0.88 μM), *p*-chloronitrobenzene (1.8 mM /3 mM /4 mM), $NaBH_4$ (20 mM), 50°C**.** The control group was carried out with ptnp (K_2PtCl_4 reduced by $NaBH_4$) as the catalyst. Note：All catalysts in the reaction contain the same amount of Pt.

The TOFs of caged Pt(wt-ptnp) catalysts

are significantly higher than that of the

control Pt catalyst (1.76 min^{-1}), which also

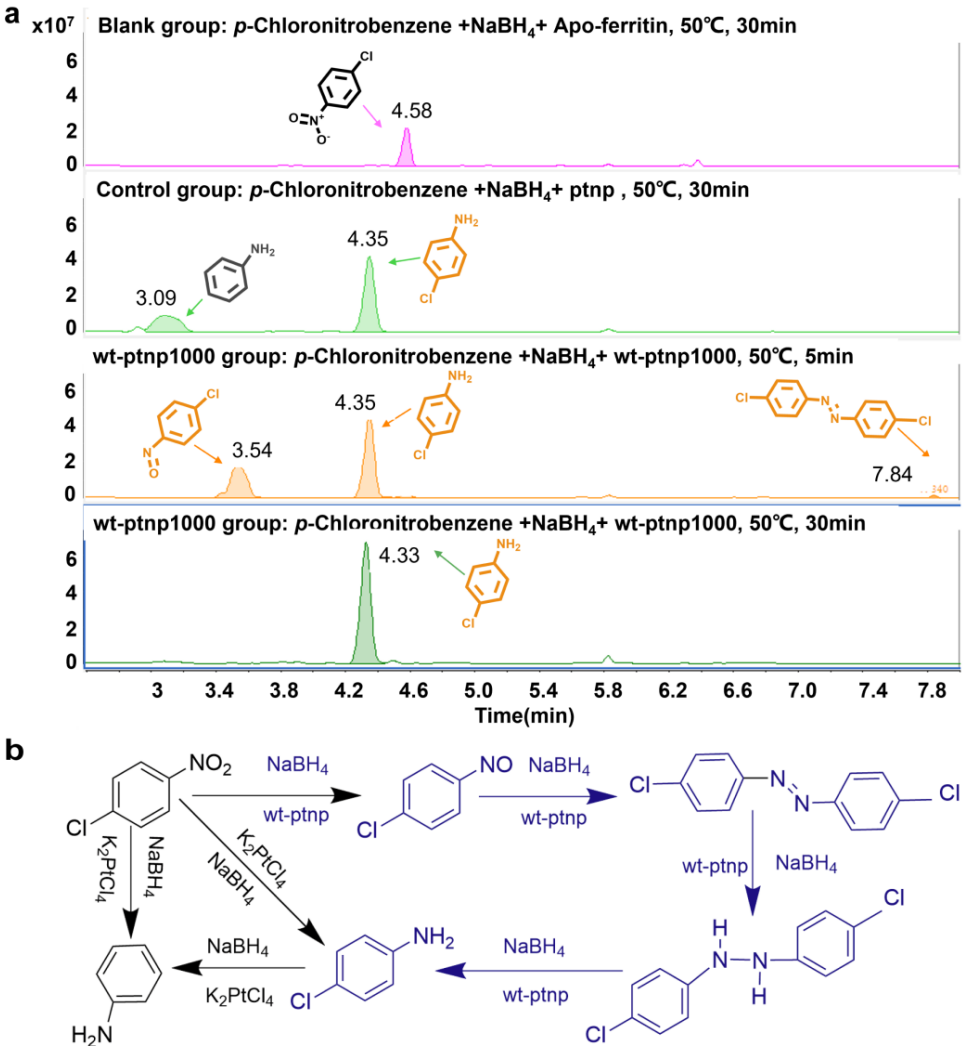

Figure 5. Mechanistic investigation of the catalytic hydrogenation of *p*-chloronitrobenzene. **a** GC-MS elution profile showing the retention time of substrate, intermediate(s) and products of the hydrogenation reactions of *p*-chlorobenzene. The X-axis represents the retention time in min and the Y-axis represents the total ion count [x 10^7]. **b** Schematic representation showing the proposed mechanistic path of *p*-chloronitrobenzene reduction by ptnp (K_2PtCl_4 reduced by $NaBH_4$) and wt-ptnp.

Table 2. Effect of substrate types on the catalytic activity of wt-ptnp1000.

Entry substrate	Catalyst	Time(min)	Conversion (%)	Selectivity (%)	Yield (%)
***p*-chloronitrobenzene**	wt-ptnp1000	30	98 ± 0.17	99 ± 0.51	98 ± 0.33
	ptnp	30	93 ± 0.02	60 ± 0.59	56 ± 0.56
***p*-bromonitrobenzene**	wt-ptnp1000	60	63 ± 0.99	99 ± 0.18	62 ± 1.09
	ptnp	60	63 ± 1.08	45 ± 0.49	29 ± 0.23
***p*-Iodonitrobenzene**	wt-ptnp1000	60	60 ± 0.47	98 ± 0.55	59 ± 0.58
	ptnp	60	54 ± 0.57	50 ± 0.70	27 ± 0.77
***o*-chloronitrobenzene**	wt-ptnp1000	30	99 ± 0.17	99 ± 0.07	99 ± 0.10
	ptnp	30	89 ± 0.08	55 ± 0.30	49 ± 0.22
***o*-bromonitrobenzene**	wt-ptnp1000	60	84 ± 0.09	99 ± 0.05	84 ± 0.29
	ptnp	60	80 ± 0.24	46 ± 0.21	36 ± 0.28
***o*-iodonitrobenzene**	wt-ptnp1000	60	81 ± 0.33	92 ± 0.49	75 ± 0.09
	ptnp	60	87 ± 0.27	53 ± 0.05	47 ± 0.10
***m*-chloronitrobenzene**	wt-ptnp1000	30	82 ± 0.41	99 ± 0.10	81 ± 0.33
	ptnp	30	81 ± 0.17	35 ± 1.91	29 ± 1.49
***m*-bromonitrobenzene**	wt-ptnp1000	60	63 ± 0.33	90±0.11	57 ± 0.22
	ptnp	60	70 ± 0.75	30 ± 0.03	21 ± 0.16
***m*-iodonitrobenzene**	wt-ptnp1000	60	52 ± 0.19	92 ± 0.41	48 ± 0.90
	ptnp	60	57 ± 0.02	23 ± 0.20	13 ± 0.12

The conversion, selectivity, and yield were determined using wt-ptnp1000 (1 μmol/L, 0.5 mL) and ptnp (K_2PtCl_4 reduced by $NaBH_4$, 1 μmol/L, 0.5 mL) to catalyze the reduction of different kinds of substrate (0.06 mol/L, 20 μL) by $NaBH_4$(0.5 mol/L, 0.1 mL) at 50°C. Note：All catalysts in the reaction contain the same amount of Pt.

suggests the influence of protein scaffold (Figure 3d and Table S2). The wt-ptnp1000 has the highest reaction yield, and the TOF, 22.80 min^{-1}, which may attribute to a smaller Pt particle size that is favorable for high activity. Moreover, a smaller particle size

may also favor electron transfer between Pt and apo-ferritin. The TOF of the reaction for wt-ptnp increases significantly as the substrate concentration increases in the range of 1.8 – 3.0 mM, and then TOF roughly stabilizes at a higher substrate concentration of 3 – 4 mM (Table S2). These results might be due to the restricted environment of the protein cage. Due to the crowding and diffusion limits of substrate/product inside the cage, the reaction might saturate at these conditions. Additionally, we have shown that apo-ferritin does not catalyze the reaction, and therefore the presence of unloaded apo-ferritin does not impact our conclusions. Moving forward, we plan to optimize the preparation process and reaction conditions to minimize the amount of unloaded apo-ferritin and improve the success rate of loading the catalyst.

Selectivity of hydrogenation catalyzed by Pt nanoparticles caged in apo-ferritin. We extended the substrate spectrum for the wt-ptnp1000, and the results showed higher selectivity and comparable conversions to ptnp (Table 2), which is because the electronic state of Pt nanoparticles loaded into apo-ferritin attenuates the electronic feedback between Pt and the benzene ring, and inhibits the occurrence of dechlorination reaction of halogenated aniline[40]. Furthermore, the results of the reaction conversion and yield show that the efficiency of the reaction of halogenated nitrobenzene with *o*-substitution is higher than that of *p*- and *m*-substituents[51] and becomes smaller as the electronegativity of the substituent decreases.

The mechanism of wt-ptnp in the hydrogenation of *p*-chloronitrobenzene. We investigated the mechanistic path of *p*-chloronitrobenzene reduction by GC-MS analysis. The result (Figure 5a) after 5 min of reaction showed that the intermediate products *p*-chloronitrosobenzene and 4,4, -dichloroazobenzene, were produced during the catalytic reaction of wt-ptnp. In contrast, the control group with ptnp (K_2PtCl_4 reduced by $NaBH_4$) as the catalyst produces aniline (Figure. 5 a and S6). We proposed a reaction route based on the intermediate and final product, as shown in Figure. 5b.

The enhanced catalytic efficacy of Pt nanoparticles caged (wt-ptnp) in apo-ferritin may be attributed to the fact that the caged Pt nanoparticles have a smaller size favorable for a higher activity[35]. Secondly, according to the XPS data, it can be found that the 4f orbital binding energy of Pt in the wt-ptnp catalyst is smaller compared with that of Pt in the control ptnp catalyst, indicating an enhanced electron acceptance. This more electron-erichened effect makes it easier for

Pt to adsorb the electron-absorbing group nitro on *p*-chloronitrobenzene and less likely to adsorb its hydrogenation product[20, 52-53]. This electron effect may also facilitate the formation of electron-rich hydrogen that is more inclined to nucleophilic attack on nitro, which can improve the hydrogenation efficiency of *p*-chloronitrobenzene and reduce the dechlorination reaction[10, 40, 54]. It is noted here that the confinement by apo-ferritin is also favorable for maintaining the Pt particle size, structure, and, thus, activity, as discussed by Z. Varpness in the case of platinum nanoparticles in heat shock protein cage[43].

To summarize the above information, it is clear that apo-ferritin provides domain-limited space, which can not only control the preparation of smaller-size Pt nanocatalysts but also modify the electronic structure of Pt by interacting with the metal. The smaller size and electronic structure effect that apo-ferritin brings to Pt nanocatalysts are essential to promote high performance. It would be interesting to explore if apo-ferritin has favorable and differentiated interactions with substrate and product[50], thereby enhancing substrate uptake and product release through molecular dynamics simulations and computational chemistry in the future .

CONCLUSIONS

In contrast to conventional high-temperature and high-pressure processes and reactions for preparing noble metal nanoparticles, we used inexpensive ferritin, which functions as both a carrier and a microreactor, to prepare structurally controlled platinum metal nanocatalysts under mild room temperature conditions. Since the synthesis process occurred in the inner cavity of ferritin, relatively small-size Pt metal nanocatalysts (2-3 nm) could be synthesized, which showed no precipitation after two months of storage in buffer at 4°C, and their activity was almost unaffected, with good stability, dispersibility, and good biocompatibility. Furthermore, in terms of catalytic performance, the catalyst can achieve the selective conversion of *p*-chloronitrobenzene to *p*-chloroaniline in 30 min at 50°C, effectively inhibiting the occurrence of dechlorination side effects and maintaining high activity while having high selectivity. This research makes up for the complicated preparation method, harsh reaction conditions, easy agglomeration, and low selectivity of the existing catalysts for the hydrogenation and reduction of *p*-chloronitrobenzene. In addition, the catalyst also showed excellent selectivity and a good activity for other halogenated nitrobenzenes. Combined with the information of our

proposed clear reaction pathway and catalytic mechanism, the results of this study will provide a reference for the rational design of protein-based metal nanocatalysts, which can be extended to other metal catalysts and catalytic reactions, promising to expand more possibilities of metal nanocatalysis.

ASSOCIATED CONTENT

Supporting Information. The Supporting Information is available free of charge at https://pubs.acs.org/doi/xx.xx/xxx

"Additional experimental details, materials, and methods, including TEM figures of catalysts (DOC)".

AUTHOR INFORMATION

Corresponding Authors

Diannan Lu - Department of Chemical Engineering, Tsinghua University, Beijing 100084, China. E-mail: ludiannan@tsinghua.edu.cn

Takafumi Ueno - School of Life Science and Technology, Tokyo Institute of Technology, Nagatsuta-cho 4259, Midori-ku, Yokohama 226-8501, Japan. Email: tueno@bio.titech.ac.jp

Zheng Liu - Department of Chemical Engineering, Tsinghua University, Beijing 100084, China. E-mail: liuzheng@tsinghua.edu.cn

Authors

Yinhuan Zhou - Department of Chemical Engineering, Tsinghua University, Beijing 100084, China. E-mail: zhou-yh20@mails.tsinghua.edu.cn

Yilin Zheng - Institute of Biopharmaceutical and Health Engineering, Shenzhen International Graduate School, Tsinghua University, Shenzhen 518055, China. zhengyl22@mails.tsinghua.edu.cn

Chenlin Lu - Department of Chemical Engineering, Tsinghua University, Beijing 100084, China. E-mail: lucl17@outlook.com

Basudev Maity - School of Life science and Technology, Tokyo Institute of Technology, Nagatsuta-cho 4259, Midori-ku, Yokohama 226-8501, Japan. Email: basudev@bio.titech.ac.jp

Yakui Chen - Department of Chemical Engineering, Tsinghua University, Beijing 100084, China. E-mail:chenyk21@mails.tsinghua.edu.cn

Author Contributions

Yinhuan Zhou: investigation, conceptualization, methodology, data curation, formal analysis, writing – original

draft, writing – review & editing. Yilin Zheng: investigation, formal analysis, writing – original draft. Chenlin Lu: reviewing & editing. Basudev Maity, Yakui Chen: investigation, writing – original draft, reviewing & editing. Zheng Liu, Takafumi Ueno, Diannan Lu: supervision, conceptualization, project administration, funding acquisition, writing – reviewing & editing.

ACKNOWLEDGMENT

This work was supported by the National Key Research and Development Program of China Grant no. 2021YFC2102801 and the Chinese National Natural Science Foundation under Grant No. 21878175.

ABBREVIATIONS

ICP-MS inductively coupled plasma mass spectrometry; BCA, bicinchoninic acid); TEM, transmission emission microscopy; XPS, X-ray photoelectron spectroscopy; GC-MS, Gas chromatography mass spectrometry.

REFERENCES

(1) Blaser, H. U.; Malan, C.; Pugin, B.; Spindler, F.; Steiner, H.; Studer, M. Selective Hydrogenation for Fine Chemicals: Recent Trends and New Developments. *ChemInform* **2003,** *345*, 103-151.
(2) Khattab, T. A.; Gaffer, H. E. Synthesis and application of novel tricyanofuran hydrazone dyes as sensors for detection of microbes. *COLORATION TECHNOLOGY* **2016,** *132* (6), 460-465, DOI: 10.1111/cote.12233.
(3) Jingmei, Y.; Rui, Z. Research Progress in Preparation of Aromatic Amine via Reduction of Aromatic Nitro Compounds. *Chemical Research* **2010,** *21* (01), 96-101, DOI: 10.14002/j.hxya.2010.01.007.
(4) Huang, P.; wang, P.; Huang, L. Development of the preparation methods for aromatic amine by reduction of aromatic nitro compounds. *Journal of Nanjing Tech University(Natural Science Edition)* **2007,** (04), 101-106.
(5) zhou, Y.; Zhu, J.; Zhao, C. Progress in preparation of aromatic amines by reduction. *Applied Chemical Industry* **2017,** *46* (04), 784-787+793, DOI: 10.16581/j.cnki.issn1671-3206.20170222.023.
(6) Corma, A.; Serna, P. Chemoselective Hydrogenation of Nitro Compounds with Supported Gold Catalysts. *Science* **2006,** *313* (5785), 332-334, DOI: doi:10.1126/science.1128383.
(7) Zhang, Q.; Bu, J.; Wang, J.; Sun, C.; Zhao, D.; Sheng, G.; Xie, X.; Sun, M.; Yu, L. Highly Efficient Hydrogenation of Nitrobenzene to Aniline over Pt/CeO₂ Catalysts: The Shape Effect of the Support and Key Role of Additional Ce³⁺ Sites. *ACS Catalysis* **2020,** *10* (18), 10350-10363, DOI: 10.1021/acscatal.0c02730.
(8) Boymans, E. H.; Witte, P. T.; Vogt, D. A study on the selective hydrogenation of nitroaromatics to N -arylhydroxylamines using a supported Pt nanoparticle catalyst. *Catalysis Science & Technology* **2014,** *5* (1), 176-183.
(9) Liu, X.; Li, H.-Q.; Ye, S.; Liu, Y.; He, H.; Cao, Y. Gold-catalyzed direct hydrogenative coupling of nitroarenes to synthesize aromatic azo compounds. *Angewandte Chemie* **2014,** *53* (29), 7624-7628.
(10) Zequn, Y.; Jie, Z.; Yan, Z.; Wei, S.; Libo, S. Research progress of catalysts for reduction of p-chloronitrobenzene with high

selectivity. *Petrochemical Technology* **2021,** *50*, 1167-1173.
(11) Sheng, Y. Catalyst for the reduction of nitroarenes. PH.D, Shanghai University, 2020.
(12) Jagadeesh, R. V.; Murugesan, K.; Alshammari, A. S.; Neumann, H.; Pohl, M.-M.; Radnik, J.; Beller, M. MOF-derived cobalt nanoparticles catalyze a general synthesis of amines. *Science* **2017,** *358* (6361), 326-332, DOI: doi:10.1126/science.aan6245.
(13) Li, Y.; Zhou, Y.-X.; Ma, X. Y.; Jiang, H. L. A metal-organic framework-templated synthesis of γ-Fe2O3 nanoparticles encapsulated in porous carbon for efficient and chemoselective hydrogenation of nitro compounds. *Chemical communications* **2016,** *52* 4199-4202.
(14) Aditya, T.; Pal, A.; Pal, T. Nitroarene reduction: a trusted model reaction to test nanoparticle catalysts. *Chemical communications* **2015,** *51*, 9410-9431.
(15) Cui, X.; Zhou, X.; Dong, Z. Ultrathin γ-Fe2O3 nanosheets as a highly efficient catalyst for the chemoselective hydrogenation of nitroaromatic compounds. *Catalysis Communications* **2018,** *107*, 57-61, DOI: https://doi.org/10.1016/j.catcom.2018.01.015.
(16) Pogorelić, I.; Filipan-Litvić, M.; Merkaš, S.; Ljubić, G.; Cepanec, I.; Litvić, M. Rapid, efficient and selective reduction of aromatic nitro compounds with sodium borohydride and Raney nickel. *Journal of Molecular Catalysis A: Chemical* **2007,** *274* (1), 202-207, DOI: https://doi.org/10.1016/j.molcata.2007.05.020.
(17) Cheruvathoor Poulose, A.; Zoppellaro, G.; Konidakis, I.; Serpetzoglou, E.; Stratakis, E.; Tomanec, O.; Beller, M.; Bakandritsos, A.; Zboril, R. Fast and selective reduction of nitroarenes under visible light with an earth-abundant plasmonic photocatalyst. *Nat Nanotechnol* **2022,** *17*, 485-492, DOI: 10.1038/s41565-022-01087-3.
(18) Serna, P.; Corma, A. Transforming Nano Metal Nonselective Particulates into Chemoselective Catalysts for Hydrogenation of Substituted Nitrobenzenes. *ACS Catalysis* **2015,** *5*, 7114-7121.
(19) Coq, B.; Tijani, A.; Figuéras, F. Particle size effect on the kinetics of p-chloronitrobenzene hydrogenation over platinum/alumina catalysts. *Journal of Molecular Catalysis* **1991,** *68* (3), 331-345, DOI: https://doi.org/10.1016/0304-5102(91)80091-G.
(20) Shi, W.; Zhang, B.; Lin, Y.; Wang, Q.; Zhang, Q.; Su, D. S. Enhanced Chemoselective Hydrogenation through Tuning the Interaction between Pt Nanoparticles and Carbon Supports: Insights from Identical Location Transmission Electron Microscopy and X-ray Photoelectron Spectroscopy. *ACS Catalysis* **2016,** *6* (11), 7844-7854, DOI: 10.1021/acscatal.6b02207.
(21) Blaser, H.-U.; Steiner, H.; Studer, M. Selective Catalytic Hydrogenation of Functionalized Nitroarenes: An Update. *ChemCatChem* **2009,** *1* (2), 210-221, DOI: 10.1002/cctc.200900129.
(22) Guan, Q.; Zhu, C.; Lin, Y.; Vovk, E. I.; Zhou, X.; Yang, Y.; Yu, H.; Cao, L.; Wang, H.; Zhang, X.; Liu, X.; Zhang, M.; Wei, S.; Li, W.-X.; Lu, J. Bimetallic monolayer catalyst breaks the activity–selectivity trade-off on metal particle size for efficient chemoselective hydrogenations. *Nature Catalysis* **2021,** *4* (10), 840-849, DOI: 10.1038/s41929-021-00679-x.
(23) Liu, M.; Tang, W.; Xie, Z.; Yu, H.; Yin, H.; Xu, Y.; Zhao, S.; Zhou, S. Design of Highly Efficient Pt-SnO2 Hydrogenation Nanocatalysts using Pt@Sn Core–Shell Nanoparticles. *ACS Catalysis* **2017,** *7* (3), 1583-1591, DOI: 10.1021/acscatal.6b03109.
(24) Wang, S.; Dai, J.; Shi, Z.; Xiong, Z.; Zhang, Z.; Qiu, S.; Wang, R. Hollow Nano-Mesosilica Spheres Containing Rhodium Nanoparticles Supported on Nitrogen-Doped Carbon: An Efficient Catalyst for the Reduction of Nitroarenes under Mild

Conditions. *ChemPlusChem* **2020,** *85* (1), 247-253.
(25) Zhang, X.; Gu, Q.; Ma, Y.; Guan, Q.; Jin, R.; Wang, H.; Yang, B.; Lu, J. Support-Induced unusual size dependence of Pd catalysts in chemoselective hydrogenation of para-chloronitrobenzene. *Journal of Catalysis* **2021,** *400*, 173-183, DOI: https://doi.org/10.1016/j.jcat.2021.06.002.
(26) Axet, M. R.; Conejero, S.; Gerber, I. C. Ligand Effects on the Selective Hydrogenation of Nitrobenzene to Cyclohexylamine Using Ruthenium Nanoparticles as Catalysts. *ACS Applied Nano Materials* **2018,** *1* (10), 5885-5894, DOI: 10.1021/acsanm.8b01549.
(27) Wang, S.; Wu, C.; Yu, H.; Li, T.; Yan, X.; Yan, B.; Yin, H. Fabrication of Ir-CoOx@mesoporous SiO2 Nanoreactors for Selective Hydrogenation of Substituted Nitroaromatics. *ACS Applied Materials & Interfaces* **2020,** *12* (8), 9966-9976, DOI: 10.1021/acsami.9b21077.
(28) Wang, C.; Mao, S.; Wang, Z.; Chen, Y.; Yuan, W.; Ou, Y.; Zhang, H.; Gong, Y.; Wang, Y.; Mei, B.; Jiang, Z.; Wang, Y. Insight into Single-Atom-Induced Unconventional Size Dependence over CeO2-Supported Pt Catalysts. *Chem* **2020,** *6* (3), 752-765, DOI: 10.1016/j.chempr.2019.12.029.
(29) Sun, Z.; Zhao, Y.; Xie, Y.; Tao, R.; Zhang, H.; Huang, C.; Liu, Z. The solvent-free selective hydrogenation of nitrobenzene to aniline: an unexpected catalytic activity of ultrafine Pt nanoparticles deposited on carbon nanotubes. *Green Chemistry* **2010,** *12* (6), 1007-1011, DOI: 10.1039/c002391d.
(30) Zhou, P.; Li, N.; Chao, Y.; Zhang, W.; Lv, F.; Wang, K.; Yang, W.; Gao, P.; Guo, S. Thermolysis of Noble Metal Nanoparticles into Electron-Rich Phosphorus-Coordinated Noble Metal Single Atoms at Low Temperature. *Angew Chem Int Ed Engl* **2019,** *58* (40), 14184-14188, DOI: 10.1002/anie.201908351.
(31) Liu, J.; He, S.; Li, C.; Wang, F.; Wei, M.; Evans, D. G.; Duan, X. Confined synthesis of ultrafine Ru–B amorphous alloy and its catalytic behavior toward selective hydrogenation of benzene. *Journal of Materials Chemistry A* **2014,** *2* (20), 7570-7577, DOI: 10.1039/c4ta00023d.
(32) Xue, Y.; Huang, B.; Yi, Y.; Guo, Y.; Zuo, Z.; Li, Y.; Jia, Z.; Liu, H.; Li, Y. Anchoring zero valence single atoms of nickel and iron on graphdiyne for hydrogen evolution. *Nat Commun* **2018,** *9* (1), 1460, DOI: 10.1038/s41467-018-03896-4.
(33) Zhang, L.; Laug, L.; Münchgesang, W.; Pippel, E.; Gösele, U.; Brandsch, M.; Knez, M. Reducing Stress on Cells with Apoferritin-Encapsulated Platinum Nanoparticles. *Nano Letters* **2010,** *10* (1), 219-223, DOI: 10.1021/nl903313r.
(34) Bode, S. A.; Bode, S. A.; Bode, S. A.; Bode, S. A. Reactions inside nanoscale protein cages. *Nanoscale* **2011,** *3* (6), 2376-2389.
(35) Fan, J.; Yin, J.-J.; Ning, B.; Wu, X.; Hu, Y.; Ferrari, M.; Anderson, G. J.; Wei, J.; Zhao, Y.; Nie, G. Direct evidence for catalase and peroxidase activities of ferritin–platinum nanoparticles. *Biomaterials* **2011,** *32* (6), 1611-1618, DOI: https://doi.org/10.1016/j.biomaterials.2010.11.004.
(36) Maity, B.; Hishikawa, Y.; Lu, D.; Ueno, T. Recent progresses in the accumulation of metal ions into the apo-ferritin cage: Experimental and theoretical perspectives. *Polyhedron* **2019,** *172*, 104-111, DOI: 10.1016/j.poly.2019.03.048.
(37) Ueno, T.; Suzuki, M.; Goto, T.; Matsumoto, T.; Nagayama, K.; Watanabe, Y. Size-Selective Olefin Hydrogenation by a Pd Nanocluster Provided in an Apo-Ferritin Cage. *Angewandte Chemie* **2004,** *116* (19), 2581-2584, DOI: 10.1002/ange.200353436.
(38) Fan, K.; Cao, C.; Pan, Y.; Lu, D.; Yang, D.; Feng, J.; Song, L.; Liang, M.; Yan, X. Magnetoferritin nanoparticles for targeting

and visualizing tumour tissues. *Nature Nanotechnology* **2012,** *7* (7), 459-464, DOI: 10.1038/nnano.2012.90.
(39) Suzuki, M.; Abe, M.; Ueno, T.; Abe, S.; Goto, T.; Toda, Y.; Akita, T.; Yamada, Y.; Watanabe, Y. Preparation and catalytic reaction of Au/Pd bimetallic nanoparticles in apo-ferritin. *Chem Commun (Camb)* **2009,** (32), 4871-4873, DOI: 10.1039/b908742g.
(40) Zhang, J.; Wang, Y.; Ji, H.; Wei, Y.; Wu, N.; Zuo, B.; Wang, Q. Magnetic nanocomposite catalysts with high activity and selectivity for selective hydrogenation of ortho-chloronitrobenzene. *Journal of Catalysis* **2005,** *229* (1), 114-118, DOI: 10.1016/j.jcat.2004.09.029.
(41) Oksana Kasyutich, A. I., Annarita Fiorillo, Dragomir Tatchev, Armin Hoell, and Pierpaolo Ceci. Silver Ion Incorporation and Nanoparticle Formation inside the Cavity of Pyrococcus furiosus Ferritin: Structural and Size-Distribution Analyses. *J Am Chem Soc* **2010,** *132*, 3621-3627.
(42) Maity, B.; Fujita, K.; Ueno, T. Use of the confined spaces of apo-ferritin and virus capsids as nanoreactors for catalytic reactions. *Curr Opin Chem Biol* **2015,** *25*, 88-97, DOI: 10.1016/j.cbpa.2014.12.026.
(43) Varpness, Z.; Peters, J. W.; Young, M.; Douglas, T. Biomimetic Synthesis of a H2 Catalyst Using a Protein Cage Architecture. *Nano Letters* **2005,** *5* (11), 2306-2309, DOI: 10.1021/nl0517619.
(44) Prastaro, A.; Ceci, P.; Chiancone, E.; Boffi, A.; Cirilli, R.; Colone, M.; Fabrizi, G.; Stringaro, A.; Cacchi, S. Suzuki-Miyaura cross-coupling catalyzed by protein-stabilized palladium nanoparticles under aerobic conditions in water: application to a one-pot chemoenzymatic enantioselective synthesis of chiral biaryl alcohols. *Green Chemistry* **2009,** *11* (12), 1929-1932, DOI: 10.1039/b915184b.
(45) Moore, W. J.; Pauling, L. C. The Crystal Structures of the Tetragonal Monoxides of Lead, Tin, Palladium, and Platinum. *Journal of the American Chemical Society* **1941,** *63*, 1392-1394.
(46) Kumar, J.; Saxena, R. Formation of NaCl- and Cu2O-type oxides of platinum and palladium on carbon and alumina support films. *Journal of the Less Common Metals* **1989,** *147* (1), 59-71, DOI: https://doi.org/10.1016/0022-5088(89)90148-3.
(47) Wang, Z.; Wang, C.; Mao, S.; Lu, B.; Chen, Y.; Zhang, X.; Chen, Z.; Wang, Y. Decoupling the electronic and geometric effects of Pt catalysts in selective hydrogenation reaction. *Nat Commun* **2022,** *13* (1), 3561, DOI: 10.1038/s41467-022-31313-4.
(48) Wang, Q.; Wang, X.; Chen, C.-H.; Yang, X.; Huang, Y. B.; Cao, R. Defective Pt nanoparticles encapsulated in mesoporous metal-organic frameworks for enhanced catalysis. *Chemical communications* **2018,** *54 64*, 8822-8825.
(49) Lykhach, Y.; Kozlov, S. M.; Skala, T.; Tovt, A.; Stetsovych, V.; Tsud, N.; Dvorak, F.; Johanek, V.; Neitzel, A.; Myslivecek, J.; Fabris, S.; Matolin, V.; Neyman, K. M.; Libuda, J. Counting electrons on supported nanoparticles. *Nat Mater* **2016,** *15* (3), 284-288, DOI: 10.1038/nmat4500.
(50) Coq, B.; Figueras, F. Structure–activity relationships in catalysis by metals: some aspects of particle size, bimetallic and supports effects. *Coordination Chemistry Reviews* **1998,** *178-180*, 1753-1783, DOI: https://doi.org/10.1016/S0010-8545(98)00058-7.
(51) Cardenas-Lizana, F.; Gomez-Quero, S.; Keane, M. A. Exclusive production of chloroaniline from chloronitrobenzene over Au/TiO2 and Au/Al2O3. *ChemSusChem* **2008,** *1* (3), 215-221, DOI: 10.1002/cssc.200700105.
(52) Wang, X.; Chen, W.; Zhang, L.; Yao, T.; Liu, W.; Lin, Y.; Ju, H.; Dong, J.; Zheng, L.; Yan, W.; Zheng, X.; Li, Z.; Wang, X.; Yang, J.; He, D.; Wang, Y.; Deng, Z.; Wu, Y.; Li, Y.

Uncoordinated Amine Groups of Metal-Organic Frameworks to Anchor Single Ru Sites as Chemoselective Catalysts toward the Hydrogenation of Quinoline. *J Am Chem Soc* **2017,** *139* (28), 9419-9422, DOI: 10.1021/jacs.7b01686.
(53) Iihama, S.; Furukawa, S.; Komatsu, T. Efficient Catalytic System for Chemoselective Hydrogenation of Halonitrobenzene to Haloaniline Using PtZn Intermetallic Compound. *ACS Catalysis* **2015,** *6* (2), 742-746, DOI: 10.1021/acscatal.5b02464.
(54) Wang, Y.; Rong, Z.; Wang, Y.; Zhang, P.; Wang, Y.; Qu, J. Ruthenium nanoparticles loaded on multiwalled carbon nanotubes for liquid-phase hydrogenation of fine chemicals: An exploration of confinement effect. *Journal of Catalysis* **2015,** *329*, 95-106, DOI: 10.1016/j.jcat.2015.04.034.